Am J Transl Res 2024;16(12):7374-7384
www.ajtr.org /ISSN:1943-8141/AJTR0157736

Original Article

miR-129-5p targets HOXC10 to control BMSC adipogenesis and osteogenesis in a model of steroid-induced osteonecrosis of the femoral head

Xuezhao Li[1], Fangqiu Tian[1], Guohua Liu[1], Xiang Liu[1], Ming Fu[1], Zhiyin E[1], Cong Wang[1], Fapeng Gao[2]

[1]Department of Orthopedics, Heilongjiang Provincial Hospital, Harbin 150036, Heilongjiang, China; [2]Department of Orthopedics, Huai'an Hospital of Huai'an City, Huai'an 223200, Jiangsu, China

Received May 13, 2024; Accepted November 19, 2024; Epub December 15, 2024; Published December 30, 2024

Abstract: Background: Steroid-induced osteonecrosis of the femoral head (SONFH) is a pathological condition primarily driven by an impaired balance in the differentiation of bone marrow mesenchymal stem cells (BMSCs) into adipogenic and osteogenic lineages. This study aimed to explore the role of miR-129-5p as a regulator of SONFH progression and associated mechanisms. Methods: BMSCs were harvested from a rat SONFH model. qPCR was leveraged to assess miR-129-5p levels, while both qPCR and Western immunoblotting were utilized to evaluate HOXC10 expression. CCK8 assay was used to measure the proliferative activity of BMSCs, while their differentiation was analyzed using qPCR and Western blot. Results: SONFH was associated with reduced miR-129-5p levels. Downregulation of miR-129-5p promoted BMSC adipogenesis while inhibiting their osteogenic differentiation and enhancing their adipogenesis differentiation. Mechanistically, miR-129-5p was found to regulate these processes by targeting the expression of the HOXC10 gene. Conclusions: MiR-129-5p is downregulated in a rat SONFH model. Reduced miR-129-5p levels facilitated adipogenesis and suppressed osteogenesis in BMSCs through its inhibition of HOXC10. These findings offer novel insights into the prevention and treatment of SONFH.

Keywords: MiR-129-5p, osteogenic differentiation, adipogenic differentiation, BMSCs, HOXC10, steroid-induced osteonecrosis of the femoral head

Introduction

Osteonecrosis of the femoral head (ONFH) is an extremely disabling condition characterized by progressive femoral head collapse and the concomitant degeneration of the associated cartilage, ultimately leading to degenerative arthritis [1-3]. ONFH can result from traumatic injuries or nontraumatic causes, with steroid-induced ONFH (SONFH) being the most common nontraumatic form of this disease [4, 5]. Excessive steroid utilization disrupts lipid metabolism, leading to fat accumulation in the medullary cavity, vascular endothelial damage, and eventual blockage of blood vessels in femoral head [5]. These changes are accompanied by a shift in bone marrow mesenchymal stem cell (BMSC) differentiation, with steroids suppressing osteogenesis while favoring adipogenesis under prolonged exposure [6]. The development of SONFH significantly impairs patient quality of life. While the precise mechanisms underlying the etiology of SONFH remain to be fully clarified, various contributing factors have been implicated, including dysregulated lipid metabolism [3], intravascular coagulation [7], inflammatory activity, apoptosis [8], and the net reduction in BMSC osteogenesis [2, 9].

MicroRNAs (miRNAs), a class of 18-24 nucleotide non-coding RNAs, regulate physiological activities by either suppressing the translation or degrading mRNA targets with complementary 3'-untranslated region (3'-UTR) sequences [10, 11]. Several miRNAs have been implicated in SONFH. For instance, miR-23b-3p promotes SONFH pathogenesis by inhibiting ZNF667 [12], miR-224 influences adipogenic and osteogenic differentiation in this condition [13], and miR-486-5p targets TBX2/P21 signaling to exert protective effects [14].

https://doi.org/10.62347/CHGJ7909

While miR-129-5p has previously been identified as a promoter of osteogenic differentiation [15], its specific role in SONFH pathogenesis remains to be clarified. Therefore, this study was conducted to explore how miR-129-5p modulates BMSC osteogenesis and adipogenesis, aiming to determine its potential as a therapeutic target for SONFH intervention.

Materials and methods

Rat SONFH model establishment

Female Sprague-Dawley (SD) rats (190-220 g) from the Academy of Military Medical Sciences (Beijing, China) were housed under controlled settings (24 ± 2°C, 12 h light-dark cycle) with ad libitum access to food and water. All animal studies were conducted as per Animal Care Committee of China guidelines and were approved by Heilongjiang Provincial Hospital. Rats were randomly assigned into two groups (n=10 each), a control group and a SONFH model group. To establish the SONFH model, rats were intraperitoneally administered 20 μg/kg lipopolysaccharide (Sigma-Aldrich, Shanghai, China) for 2 days, followed by intramuscular administration of 40 mg/kg methylprednisolone (Sinopharm, China) every 24 h for 3 days [13]. Rats were euthanized by excessive inhalation of CO_2 for sample collection.

Micro-CT scanning

The right femoral head of each rat was scanned using micro-CT scanner (SkyScan1176, Bruker, Germany) and 3D reconstruction was performed. Bone parameters of femoral trabecular bone, mineral density (BMD), trabecular thickness (Tb.Th), trabecular number (Tb.N), and bone volume fraction (BV/TV), were analyzed using SkyScan software.

Isolation and culture of BMSCs

BMSCs were isolated by gradient density centrifugation and cultured in Dulbecco modified eagle's medium (DMEM, Gibco, NY, USA) containing 10% fetal bovine serum (Gibco) and 5% CO_2 at 37°C. The culture medium was replaced every three days. Once the BMSCs reached 90% fusion, they were sub-cultured into two new plates for further use.

Cell transfection

BMSCs were seeded in 6-well plates and transfected with 30 nM negative control (miR-NC mimic, or miR-NC inhibitor), miR-129-5p mimic, or miR-129-5p inhibitor with Lipofectamin RNAiMAX transfection reagent (Thermo Fisher, Tokyo, Japan) for 16 h. Samples were collected 48 hours post-transfection. The sequences of the oligonucleotides used were as follows: miR-NC mimic: UUGUACUACACAAAAGUACUG; miR-129-5p mimic: CUUUUUGCGGUCUGGGCUUGC; miR-NC inhibitor: CAGUACUUUUGUGUAGUACAA; and miR-129-5p inhibitor: GCAAGCCCAGACCGCAAAA. All oligonucleotides were purchased from MedChemExpress.

qPCR

Total RNA was extracted from BMSCs using TRIzol (Thermo Fisher) according to the manufacturer's instructions. RNA quality was assessed via absorbance measurements. For cDNA synthesis, 1 μg of RNA per sample was processed using the SuperScript RT reagent kit with gDNA Eraser (Takara) for general RNA and the miRNA first strand cDNA synthesis kit (Sangon Biotech) for miRNA-specific analyses. All qPCR analyses were performed in 10 μl reaction solution, containing 5 μl of 2× Power SYBR Green PCR Master Mix (ABI), 0.25 μl each of forward/reverse primers, 1 μg of cDNA, and dH_2O. GAPDH served as reference gene, with the $2^{-\Delta\Delta Ct}$ method was employed to determine relative gene expression. The primer sequences are provided in **Table 1**.

CCK8 assay

Cell viability was determined by CCK-8 assay (cat. no. HY-K0301; MedChemExpress). Cells were seeded into 96 well plates and cultured at 37°C and 5% CO_2. At 0, 24, 48 and 72 h, 10 μl of CCK-8 solution was added to each well. Then, the plates were incubated for an additional 4 h, and the optical density (OD) at 450 nm was measured using a microplate reader to evaluate cell viability.

Western blot

Protein extraction from BMSCs was performed using RIPA lysis buffer (Beyotime) containing 1% PMSF, and protein concentrations were

Table 1. The primer sequence for qPCR

Gene	Primer
HOXC10 forward	5'-GAACATCTGGAATCGCCTCAG-3'
HOXC10 reverse	5'-CTGCTCCGTCTTGATTTCATTG-3'
GAPDH forward	5'-AGAAGGCTGGGGCTC ATTTG-3'
GAPDH reverse	5'-AGGGGCCATCCACAGTCTTC-3'
OPN forward	5'-GAAGTTTCGCAGACCTGACAT-3'
OPN reverse	5'-GTATGCACCATTCAACTCCTCG-3'
ALP forward	5'-CCTTGGCGCCAGGAGAACCG-3'
ALP reverse	5'-GAACCCGGACTTCTGGAACC-3'
RUNX2 forward	5'-TGGTTACTGTCATGGCGGGTA-3'
RUNX2 reverse	5'-TCTCAGATCGTTGAACCTTGCTA-3'
PPARγ forward	5'-ATGTCTCACAATGCCATCAGG-3'
PPARγ reverse	5'-TCTGGGTTCAGCTGGTCGAT-3'
FABP4 forward	5'-AAGGTGAAGAGCATCATAACCCT-3'
FABP4 reverse	5'-TCACGCCTTTCATAACACATTCC-3'
LPL forward	5'-TGGCGTAGCAGGAAGTCTGA-3'
LPL reverse	5'-TGCCTCCATTGGGATAAATGTC-3'

quantified using a BCA kit (Beyotime). Samples were separated on 12% SDS-PAGE gels and transferred to PVDF membranes (Millipore). Membranes were blocked at room temperature using 5% non-fat milk in TBST for 1 h, followed by overnight incubation with primary antibodies (HOXC10 (Cell Signaling Technology), OPN (Abcam), ALP (Abcam), RUNX2 (Abcam), PPARγ (Abcam), FABP4 (Abcam), or LPL (Abcam); 1:1000) at 4°C. Membranes were then incubated with HRP-conjugated secondary antibodies (1:2000, Cell Signaling Technology) at room temperature. Protein bands were detected using ECL substrate (Millipore) and analyzed quantitatively using ImageJ software. GAPDH was used as a loading control for normalization.

Luciferase reporter analyses

To evaluate the binding of miR-129-5p to target gene 3'-UTR sequences, wild-type or mutated 3'-UTR fragments were cloned into the pmiR-RB-REPORT vector (Ribobio) using the XhoI and NotI restriction sites. These constructs were co-transfected into HEK293T cells along with miR-129-5p mimic or control constructs using Lipofectamine 3000 (Invitrogen). After 48 hours, luciferase activity was measured using a dual-luciferase reporter assay system (Promega), with Renilla luciferase serving as an internal control.

Alizarin Red staining (ARS)

BMSCs were induced osteogenic differentiation over 14 days, after which they were fixed with 4% paraformaldehyde for 15 min. The cell was stained using a 2% Alizarin Red S solution (Solarbio, Beijing, China) for 10 min to assess mineral deposition.

Oil Red O staining (ORO)

BMSCs were induced adipogenic differentiation over 14 days, followed by fixation with 4% paraformaldehyde for 15 min. The cell was stained with a 0.5% Oil Red O saturated solution (Cyagen, USA) for 10 min to evaluate lipid accumulation.

Statistical analyses

All statistical analyses were performed with GraphPad Prism 8. Results were presented as means ± standard deviations. *In vitro* assays were conducted in triplicates. Data were compared between or among groups using Student's t-test, one-way/two-way analysis of variance (ANOVA) with Dunnett post hoc test, or repeated measure ANOVA with Tukey's post hoc test. A P value of <0.05 was considered statistically significant.

Results

miR-129-5p was downregulated in SONFH model

A rat SONFH model was successfully established using methylprednisolone treatment. The resultant animals exhibited pronounced reductions in BMD, Tb.Th, Tb.N, and BV/TV compared to controls (**Figure 1A**), confirming successful model establishment. qPCR analysis revealed a marked downregulation of miR-129-5p expression in the SONFH model rats relative to controls (**Figure 1B**).

miR-129-5p downregulation suppressed BMSC osteogenesis while promoting adipogenic differentiation

To probe the role of miR-129-5p in BMSC osteogenesis or adipogenesis, BMSCs were transfected with miR-129-5p mimic or inhibitor plasmids and their corresponding controls. Transfection with miR-129-5p inhibitors and mimics

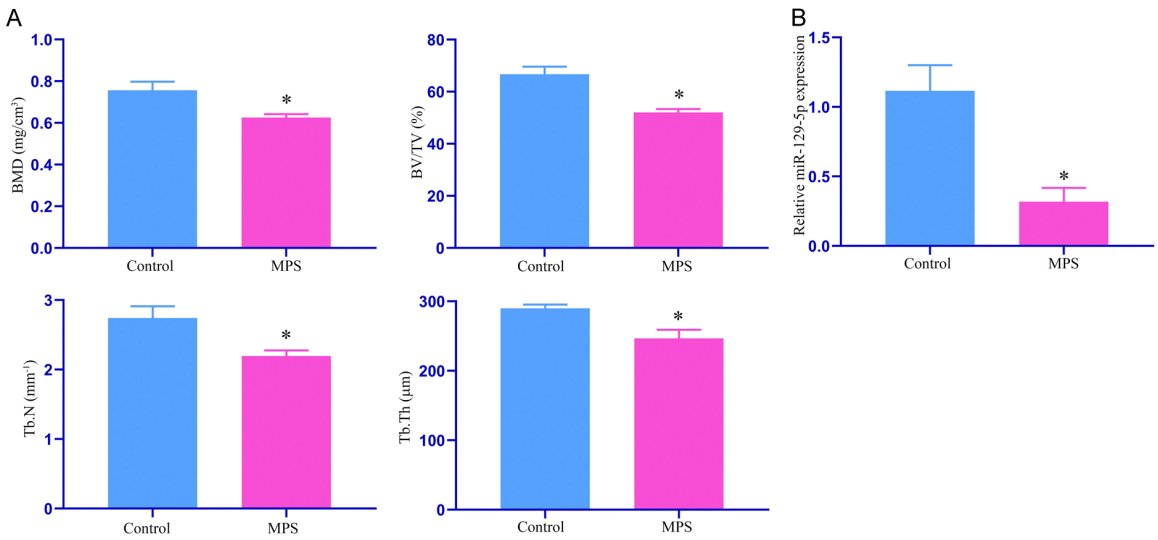

Figure 1. miR-129-5p was downregulated in SONFH rat model. A. BMD, BV/TV, Tb.Th, and Tb.N in SONFH rats; B. miR-129-5p expression in SONFH rats. BMD: bone mineral density; Tb.Th: trabecular thickness; Tb.N: trabecular number; BV/TV: bone volume fraction; MPS: methylprednisolone. *P<0.05.

led to the expected decrease and increase in miR-129-5p levels, respectively (**Figure 2A**), and respectively promoted and suppressed BMSC proliferation (**Figure 2B**). Pronounced reductions in osteogenic gene expression (OPN, ALP, RUNX2) were observed in the miR-129-5p inhibitor group, while these genes were upregulated upon miR-129-5p mimic transfection (**Figure 2C**, **2D**). ARS staining demonstrated that miR-129-5p knockdown reduced matrix mineralization in BMSCs, while miR-129-5p mimic enhanced it (**Figure 2E**). Conversely, genes associated with adipogenesis (PPARγ, FABP4, LPL) were upregulated in the miR-129-5p inhibitor group but downregulated in the mimic group (**Figure 2F**, **2G**). ORO staining revealed an increase in mature adipocytes following miR-129-5p inhibition, whereas miR-129-5p mimic suppressed adipocyte formation (**Figure 2H**).

miR-129-5p targets HOXC10 directly

TargetScan (http://www.targetscan.org) was used to predict putative miR-129-5p targets, and HOXC10 was identified as a potential target of miR-129-5p (**Figure 3A**). To validate this interaction, luciferase reporter constructs harboring either mutated or wild-type HOXC10 3'-UTR binding sites were developed (**Figure 3A**). Transfection with the miR-129-5p mimic markedly suppressed luciferase activity in cells with the wild-type OXC10 3'-UTR reporter but not in those with the mutated reporter construct (**Figure 3B**). Consistent with this observation, HOXC10 was markedly upregulated upon miR-129-5p inhibitor treatment, whereas it was downregulated in cells following miR-129-5p mimic treatment (**Figure 3C**, **3D**). These findings confirm that miR-129-5p directly targets HOXC10.

HOXC10 was upregulated in the SONFH model

HOXC10 expression was further examined in the rat SONFH model using qPCR and Western blot. Results showed significant upregulation of HOXC10 in SONFH model rats as compared to controls (**Figure 4A**, **4B**).

HOXC10 upregulation suppressed BMSC osteogenesis but promoted adipogenic differentiation

To confirm the role of HOXC10 in BMSC differentiation, HOXC10 was overexpressed using an Ad-HOXC10 construct, as confirmed by qPCR and Western blot (**Figure 5A**, **5B**). The proliferation of BMSCs was promoted in the Ad-HOXC10 group as compared to Ad-NC group (**Figure 5C**). Pronounced reductions in osteogenic gene expression (OPN, ALP, RUNX2) were observed in the Ad-HOXC10 group as compared to Ad-NC group (**Figure 5D**, **5E**). ARS staining demonstrated that overexpression of HOXC10 result-

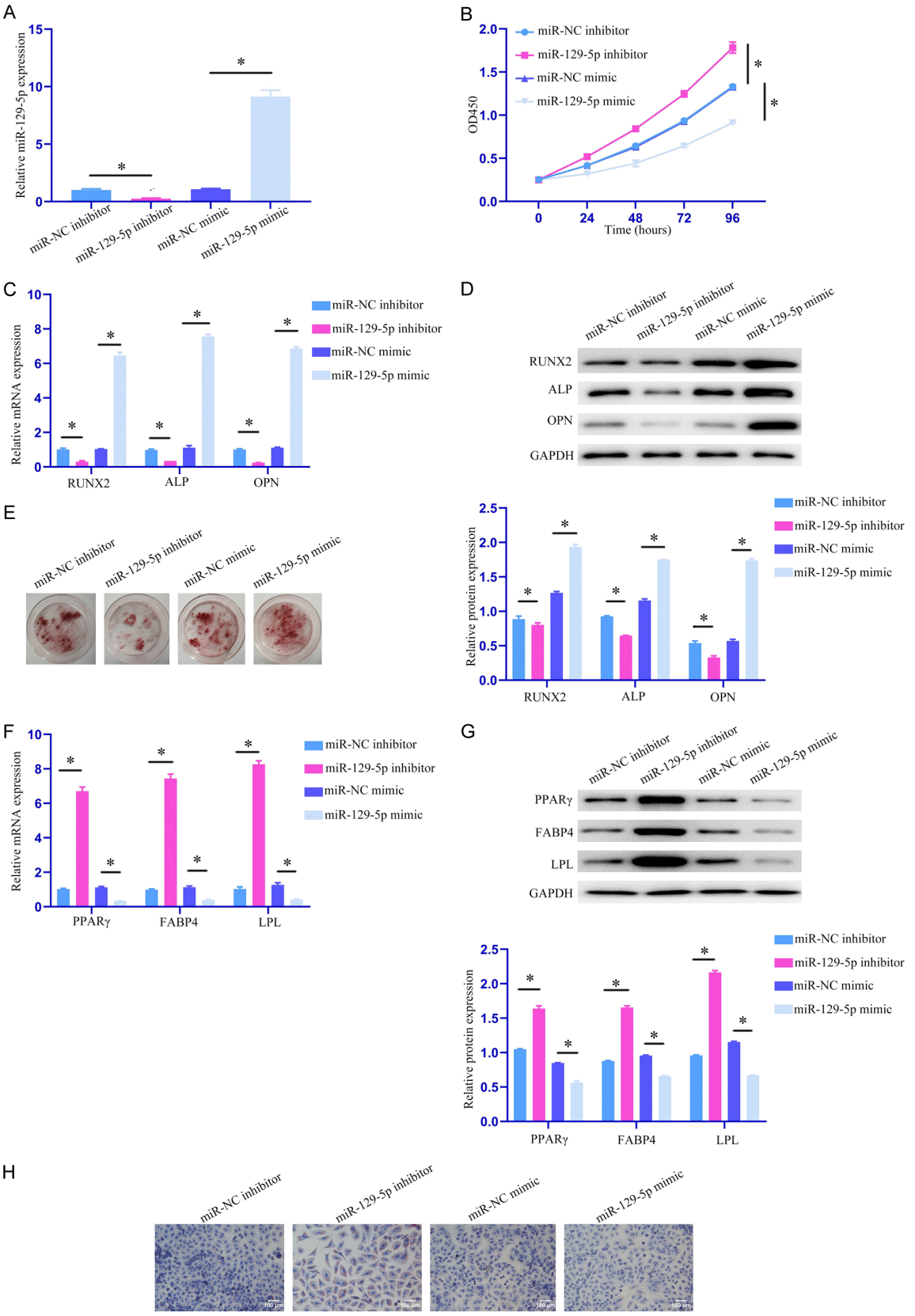

Figure 2. miR-129-5p inhibitor suppressed BMSC osteogenesis and promoted adipogenesis. (A) miR-129-5p expression quantified using qPCR; (B) BMSC proliferation detected using CCK-8 assay; (C, D) Osteogenesis-related

genes (OPN, RUNX2, and ALP) quantified using qPCR (C) and Western blot (D); (E) BMSCs in osteogenic medium determined with Alizarin red staining; (F, G) Adipogenesis-related genes (LPL, FABP4, and PPARγ) quantified using qPCR (F) and Western blot (G); (H) BMSCs in adipogenic medium detected with Oil red staining. BMSC: bone marrow mesenchymal stem cell. *P<0.05.

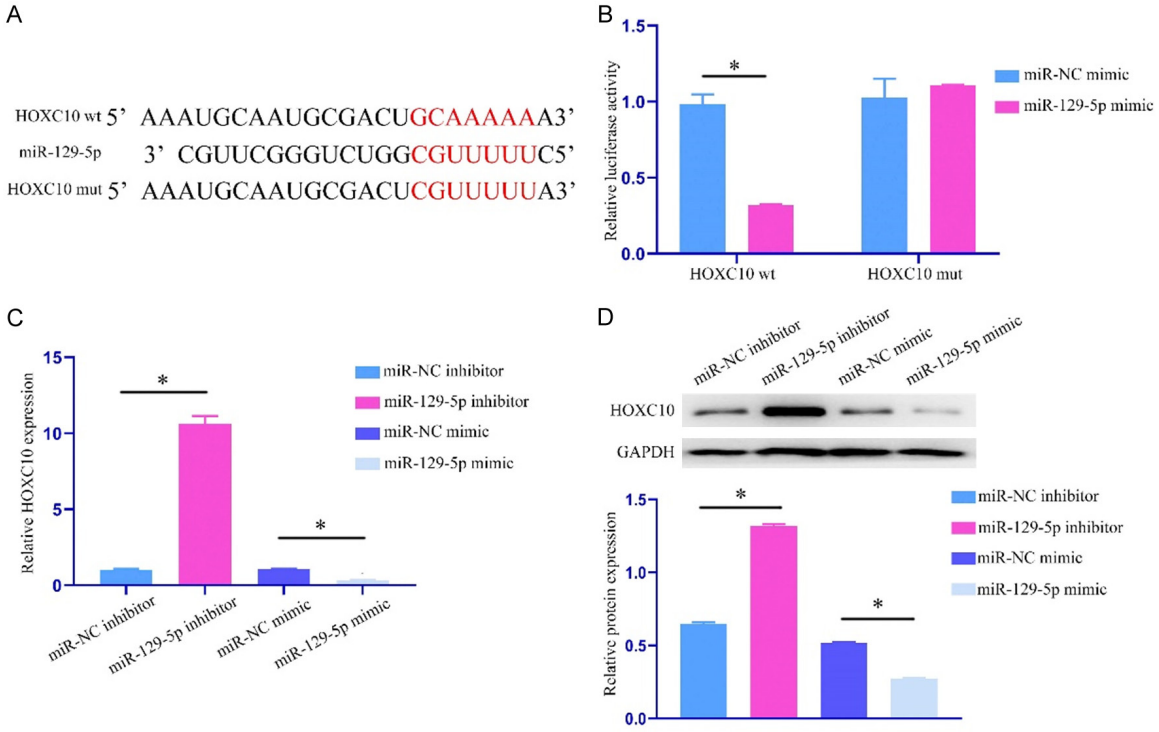

Figure 3. HOXC10 is directly targeted by miR-129-5p. (A) Targetscan identified a putative binding site between miR-129-5p and HOXC10; (B) Verification of the relationship between miR-129-5p and HOXC10 using luciferase reporter gene assay; (C, D) HOXC10 levels quantified using qPCR (C) and Western blot (D). *P<0.05.

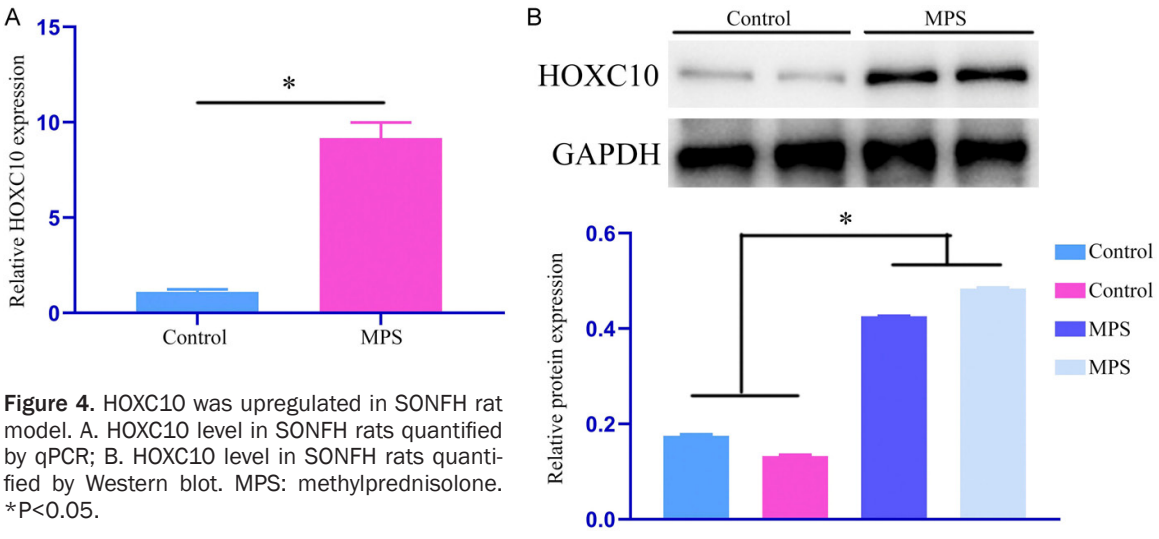

Figure 4. HOXC10 was upregulated in SONFH rat model. A. HOXC10 level in SONFH rats quantified by qPCR; B. HOXC10 level in SONFH rats quantified by Western blot. MPS: methylprednisolone. *P<0.05.

ed in the reduction of matrix mineralization in BMSC (**Figure 5F**). Conversely, genes associated with adipogenesis (PPARγ, FABP4, LPL) were significantly elevated in the Ad-HOXC10 group

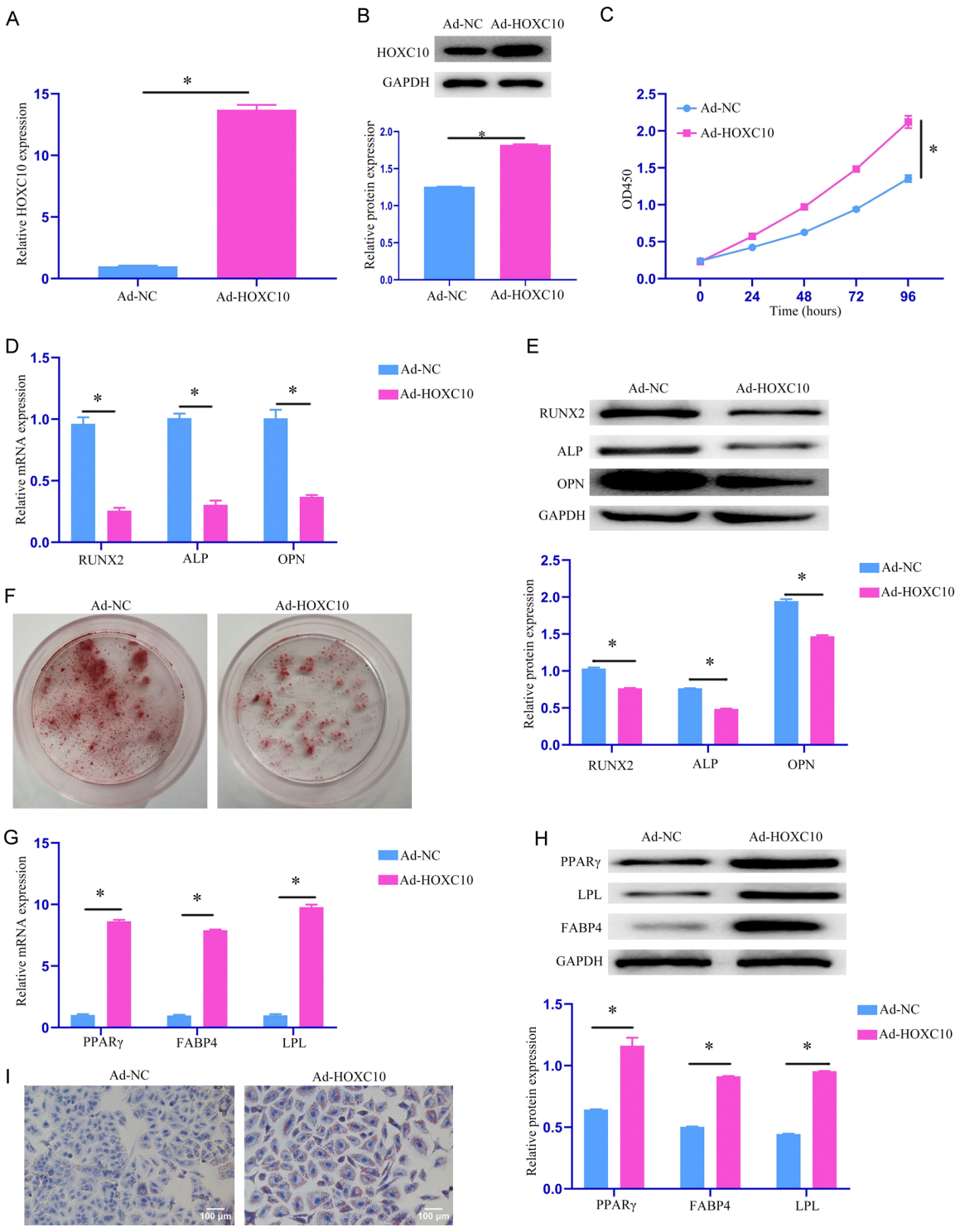

Figure 5. HOXC10 overexpression suppressed BMSC osteogenesis and promoted adipogenesis. (A, B) HOXC10 levels quantified by qPCR (A) and Western blot (B); (C) BMSC proliferation detected by CCK-8 assay; (D, E) Osteogenesis-related genes (OPN, RUNX2, and ALP) quantified using qPCR (D) and Western blot (E); (F) BMSCs in osteogenic medium observed with Alizarin red staining; (G, H) Adipogenesis-related genes (LPL, FABP4, and PPARγ) quantified using qPCR (G) and Western blot (H); (I) BMSCs in adipogenic medium observed with Oil red staining. BMSC: bone marrow mesenchymal stem cell. *P<0.05.

as compared to Ad-NC group (**Figure 5G**, **5H**). ORO staining demonstrated that HOXC10 overexpression confirmed an increase in mature adipocytes in BMSCs (**Figure 5I**).

miR-129-5p mimics promoted osteogenic differentiation and suppressed adipogenesis of BMSCs by targeting HOXC10

To confirm the role of miR-129-5p/HOXC10 axis in BMSC differentiation, a rescue experiment was conducted. The enhanced proliferation of BMSCs overexpressing HOXC10 was reversed by miR-129-5p mimic treatment (**Figure 6A**). The osteogenic gene expression (OPN, ALP, RUNX2), as well as matrix mineralization, was restored following miR-129-5p mimic treatment in BMSCs overexpressing HOXC10 (**Figure 6B-D**). Conversely, the elevated expression of adipogenic genes (PPARγ, FABP4, LPL) in HOXC10-overexpressing BMSCs was reversed by miR-129-5p mimic (**Figure 6E**, **6F**). ORO staining further confirmed that miR-129-5p mimic suppressed adipogenic differentiation in HOXC10-overexpressing BMSCs (**Figure 6G**). These findings establish that miR-129-5p promotes BMSC osteogenesis and inhibits adipogenesis by targeting HOXC10, highlighting its critical role in maintaining the balance of BMSC differentiation and its potential as a therapeutic target in SONFH.

Discussion

While steroids are integral to the treatment of many connective tissue disorders, excessive use can lead to steroid-induced osteonecrosis of the femoral head (SONFH) [16], a complex condition with an incompletely understood etiology. Efforts to better clarify the mechanisms underlying SONFH development are essential for improved diagnosis and management [17].

As small, ubiquitous noncoding RNAs, miRNAs are key regulators of numerous physiological and pathological processes [18]. Growing evidence highlights their role in modulating the differentiation of BMSCs in SONFH [19, 20]. In this study, we found miR-129-5p downregulation in SONFH, making this the first report documenting the relevance of this miRNA in SONFH. Experimental validation revealed that miR-129-5p promoted BMSC osteogenesis while inhibiting adipogenesis. Consistent with these findings, previous studies have shown the impact of miRNAs on BMSC differentiation. For instance, miR-27a has been reported as a regulator of BMSC-associated processes in SONFH [21], while miR-708 targets SMAD3 to suppress osteogenesis and to promote SONFH progression [22]. MiR-27a targets both GREM1 and PPARγ in steroid-treated rat BMSCs to enhance osteogenic differentiation while suppressing adipogenesis [17]. Our findings highlight that miR-129-5p downregulation contributes to suppressed BMSC osteogenesis and enhanced adipogenesis in SONFH.

Both autologous and allogeneic mesenchymal stem cells (MSCs) are capable of facilitating tissue regeneration in animal models and human patients [23, 24], although the precise mechanism underlying such activity remains uncertain. HOXC10 has recently established as an essential regulator of adipose tissue remodeling [25-27], while exerting opposing effects on osteogenesis. HOXC10 mutations have also been tied to patterning defects, and this protein, along with its paralogs, is involved in vertebral identity determination at transitional sites between the thoracic, lumbar, and sacral regions of the spine. Furthermore, HOXC10 plays a role in hindlimb osteogenic and chondrogenic activity, particularly influencing femoral architecture [28]. These findings align well with a role for HOXC10 in MSC osteogenesis.

HOXC10 has also been demonstrated to inhibit MSC osteogenic differentiation in previous studies [29]. Our findings corroborate these results, demonstrating that HOXC10 shifts the adipogenic-osteogenic balance of BMSC differentiation toward adipogenesis. When cells overexpressing HOXC10 were co-transfected with miR-129-5p mimic, the expression pattern of adipogenic and osteogenic genes returned to the levels similar to those observed without HOXC10 overexpression. These results highlight miR-129-5p as a potent inducer of BMSC osteogenesis through its ability to target and suppress HOXC10, thereby limiting adipogenic differentiation.

However, our work still has some limitations. First, the detailed mechanism of HOXC10 regulating BMSC needs to be further explored. Second, no drugs targeting miR-129-5p or HOXC10 were screened. Finally, apart from BMSC, it remains unclear whether miR-129-5p influences SONFH progression by regulating other cell types, such as vascular endothelial

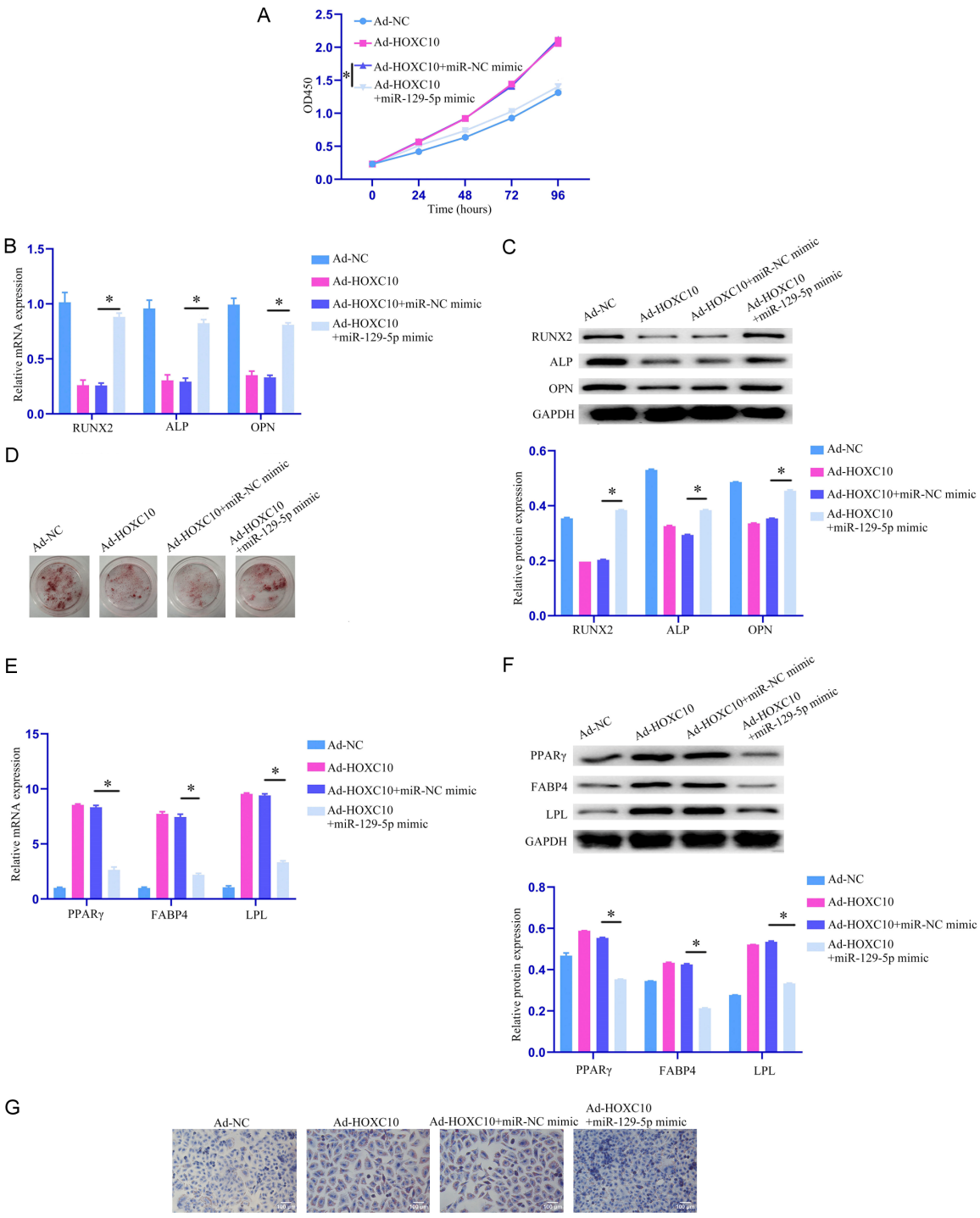

Figure 6. miR-129-5p mimics promoted osteogenesis and suppressed adipogenesis in BMSCs by targeting HOXC10. (A) BMSC proliferation detected using CCK-8 assay; (B, C) Osteogenesis-related genes (OPN, RUNX2, and ALP) quantified using qPCR (B) and Western blot (C); (D) BMSCs in osteogenic medium observed with Alizarin red staining; (E, F) Adipogenesis-related genes (LPL, FABP4, and PPARγ) quantified using qPCR (E) and Western blot (F); (G) BMSCs in adipogenic medium observed with Oil red staining. BMSC: bone marrow mesenchymal stem cell. *P<0.05.

cells and bone cells. Further research will address these limitations by including additional cell types, conducting more in-depth mechanistic studies, and exploring the therapeutic application of targeting miR-129-5p and HOXC10 in SONFH.

Conclusion

In summary, miR-129-5p is downregulated in a rat SONFH model and exerts its effects by targeting HOXC10. Specifically, reduced miR-129-5p expression was associated with enhanced adipogenesis and suppressed osteogenesis in BMSCs. These findings suggest that miR-129-5p and HOXC10 may represent viable biomarkers and therapeutic targets for the diagnosis and treatment of SONFH.

Disclosure of conflict of interest

None.

Address correspondence to: Fapeng Gao, Department of Orthopedics, Huai'an Hospital of Huai'an City, No. 19 Shanyang Avenue, Huai'an 223200, Jiangsu, China. Tel: +86-057185100293; E-mail: Gaofapeng999@163.com

References

[1] Lamb JN, Holton C, O'Connor P and Giannoudis PV. Avascular necrosis of the hip. BMJ 2019; 365: l2178.

[2] Piuzzi NS, Anis HK and Muschler GF. Osteonecrosis of the femoral head with subchondral collapse. Cleve Clin J Med 2019; 86: 511-512.

[3] Zhao J, Ma XL, Ma JX, Sun L, Lu B, Wang Y, Xing GS, Wang Y, Dong BC, Xu LY, Kuang MJ, Fu L, Bai HH, Ma Y and Jin WL. TET3 mediates alterations in the epigenetic marker 5hmC and Akt pathway in steroid-associated osteonecrosis. J Bone Miner Res 2017; 32: 319-332.

[4] Felten R, Messer L, Moreau P, Goussot R and Mahe A. Osteonecrosis of the femoral head linked to topical steroids for skin bleaching: a case report. Ann Intern Med 2014; 161: 763-764.

[5] Wang A, Ren M and Wang J. The pathogenesis of steroid-induced osteonecrosis of the femoral head: a systematic review of the literature. Gene 2018; 671: 103-109.

[6] Wang Q, Yang Q, Chen G, Du Z, Ren M, Wang A, Zhao H, Li Z, Zhang G and Song Y. LncRNA expression profiling of BMSCs in osteonecrosis of the femoral head associated with increased adipogenic and decreased osteogenic differentiation. Sci Rep 2018; 8: 9127.

[7] Fan L, Li J, Yu Z, Dang X and Wang K. Hypoxia-inducible factor prolyl hydroxylase inhibitor prevents steroid-associated osteonecrosis of the femoral head in rabbits by promoting angiogenesis and inhibiting apoptosis. PLoS One 2014; 9: e107774.

[8] Zhu ZH, Gao YS, Zeng BF and Zhang CQ. The effect of dexamethasone and hypoxic stress on MC3T3-E1 cells. Front Biosci (Landmark Ed) 2011; 16: 2747-2755.

[9] Piuzzi NS, Chahla J, Schrock JB, LaPrade RF, Pascual-Garrido C, Mont MA and Muschler GF. Evidence for the use of cell-based therapy for the treatment of osteonecrosis of the femoral head: a systematic review of the literature. J Arthroplasty 2017; 32: 1698-1708.

[10] Krol J, Loedige I and Filipowicz W. The widespread regulation of microRNA biogenesis, function and decay. Nat Rev Genet 2010; 11: 597-610.

[11] Kristensen LS, Andersen MS, Stagsted LVW, Ebbesen KK, Hansen TB and Kjems J. The biogenesis, biology and characterization of circular RNAs. Nat Rev Genet 2019; 20: 675-691.

[12] Liu Y, Zong Y, Shan H, Lin Y, Xia W, Wang N, Zhou L, Gao Y, Ma X and Jiang C. MicroRNA-23b-3p participates in steroid-induced osteonecrosis of the femoral head by suppressing ZNF667 expression. Steroids 2020; 163: 108709.

[13] Cao Y, Jiang C, Wang X, Wang H, Yan Z and Yuan H. Reciprocal effect of microRNA-224 on osteogenesis and adipogenesis in steroid-induced osteonecrosis of the femoral head. Bone 2021; 145: 115844.

[14] Zhu X, Chen D, Sun Y, Yang S, Wang W, Liu B, Gao P, Li X, Wu L, Ma S, Lin W, Ma J and Yan D. LncRNA WEE2-AS1 is a diagnostic biomarker that predicts poor prognoses in patients with glioma. BMC Cancer 2023; 23: 120.

[15] Valenti MT, Deiana M, Cheri S, Dotta M, Zamboni F, Gabbiani D, Schena F, Dalle Carbonare L and Mottes M. Physical exercise modulates miR-21-5p, miR-129-5p, miR-378-5p, and miR-188-5p expression in progenitor cells promoting osteogenesis. Cells 2019; 8: 742.

[16] Yue J, Wan F, Zhang Q, Wen P, Cheng L, Li P and Guo W. Effect of glucocorticoids on miRNA expression spectrum of rat femoral head microcirculation endothelial cells. Gene 2018; 651: 126-133.

[17] Gu C, Xu Y, Zhang S, Guan H, Song S, Wang X, Wang Y, Li Y and Zhao G. miR-27a attenuates adipogenesis and promotes osteogenesis in steroid-induced rat BMSCs by targeting PPARgamma and GREM1. Sci Rep 2016; 6: 38491.

[18] Kapinas K and Delany AM. MicroRNA biogenesis and regulation of bone remodeling. Arthritis Res Ther 2011; 13: 220.

[19] Wang B, Yu P, Li T, Bian Y and Weng X. MicroRNA expression in bone marrow mesenchymal stem cells from mice with steroid-induced osteonecrosis of the femoral head. Mol Med Rep 2015; 12: 7447-7454.

[20] Wang A, Ren M, Song Y, Wang X, Wang Q, Yang Q, Liu H, Du Z, Zhang G and Wang J. MicroRNA expression profiling of bone marrow mesenchymal stem cells in steroid-induced osteonecrosis of the femoral head associated with osteogenesis. Med Sci Monit 2018; 24: 1813-1825.
[21] Cui Y, Huang T, Zhang Z, Yang Z, Hao F, Yuan T and Zhou Z. The potential effect of BMSCs with miR-27a in improving steroid-induced osteonecrosis of the femoral head. Sci Rep 2022; 12: 21051.
[22] Hao C, Yang S, Xu W, Shen JK, Ye S, Liu X, Dong Z, Xiao B and Feng Y. MiR-708 promotes steroid-induced osteonecrosis of femoral head, suppresses osteogenic differentiation by targeting SMAD3. Sci Rep 2016; 6: 22599.
[23] Cao Y, Liu Z, Xie Y, Hu J, Wang H, Fan Z, Zhang C, Wang J, Wu CT and Wang S. Adenovirus-mediated transfer of hepatocyte growth factor gene to human dental pulp stem cells under good manufacturing practice improves their potential for periodontal regeneration in swine. Stem Cell Res Ther 2015; 6: 249.
[24] Chen FM, Gao LN, Tian BM, Zhang XY, Zhang YJ, Dong GY, Lu H, Chu Q, Xu J, Yu Y, Wu RX, Yin Y, Shi S and Jin Y. Treatment of periodontal intrabony defects using autologous periodontal ligament stem cells: a randomized clinical trial. Stem Cell Res Ther 2016; 7: 33.
[25] Brune JE, Kern M, Kunath A, Flehmig G, Schon MR, Lohmann T, Dressler M, Dietrich A, Fasshauer M, Kovacs P, Stumvoll M, Bluher M and Kloting N. Fat depot-specific expression of HOXC9 and HOXC10 may contribute to adverse fat distribution and related metabolic traits. Obesity (Silver Spring) 2016; 24: 51-59.
[26] Lim YC, Chia SY, Jin S, Han W, Ding C and Sun L. Dynamic DNA methylation landscape defines brown and white cell specificity during adipogenesis. Mol Metab 2016; 5: 1033-1041.
[27] Ferrannini G, Namwanje M, Fang B, Damle M, Li D, Liu Q, Lazar MA and Qiang L. Genetic backgrounds determine brown remodeling of white fat in rodents. Mol Metab 2016; 5: 948-958.
[28] Hostikka SL, Gong J and Carpenter EM. Axial and appendicular skeletal transformations, ligament alterations, and motor neuron loss in Hoxc10 mutants. Int J Biol Sci 2009; 5: 397-410.
[29] Li G, Han N, Yang H, Wang L, Lin X, Diao S, Du J, Dong R, Wang S and Fan Z. Homeobox C10 inhibits the osteogenic differentiation potential of mesenchymal stem cells. Connect Tissue Res 2018; 59: 201-211.